

26 May 2010, 4:45 pm - 6:45 pm

Influence of Soil Nonlinearities on Dynamic Soil-Structure Interaction

Ali Gandomzadeh

Université Paris-Est, Laboratoire Central des Ponts et Chaussées (LCPC), France

Luca Lenti

Laboratoire Central des Ponts et Chaussées (LCPC), France

Maria Paola Santisi d'Avila

Université Paris-Est, Laboratoire Central des Ponts et Chaussées (LCPC), France

Fabian Bonilla

Institute for Radiological Protection and Nuclear Safety (IRSN), France

Jean-François Semblat

Laboratoire Central des Ponts et Chaussées (LCPC), France

Follow this and additional works at: <https://scholarsmine.mst.edu/icrageesd>



Part of the [Geotechnical Engineering Commons](#)

Recommended Citation

Gandomzadeh, Ali; Lenti, Luca; d'Avila, Maria Paola Santisi; Bonilla, Fabian; and Semblat, Jean-François, "Influence of Soil Nonlinearities on Dynamic Soil-Structure Interaction" (2010). *International Conferences on Recent Advances in Geotechnical Earthquake Engineering and Soil Dynamics*. 27.

<https://scholarsmine.mst.edu/icrageesd/05icrageesd/session05/27>



This work is licensed under a [Creative Commons Attribution-Noncommercial-No Derivative Works 4.0 License](#).

This Article - Conference proceedings is brought to you for free and open access by Scholars' Mine. It has been accepted for inclusion in International Conferences on Recent Advances in Geotechnical Earthquake Engineering and Soil Dynamics by an authorized administrator of Scholars' Mine. This work is protected by U. S. Copyright Law. Unauthorized use including reproduction for redistribution requires the permission of the copyright holder. For more information, please contact scholarsmine@mst.edu.



Fifth International Conference on

Recent Advances in Geotechnical Earthquake Engineering and Soil Dynamics and Symposium in Honor of Professor I.M. Idriss

May 24-29, 2010 • San Diego, California

INFLUENCE OF SOIL NONLINEARITIES ON DYNAMIC SOIL-STRUCTURE INTERACTION

Ali Gandomzadeh, PhD student, Université Paris-Est, Laboratoire Central des Ponts et Chaussées (LCPC), 58 Bd Lefebvre 75732 Cedex 15 Paris (France), ali.gandomzadeh@lcpc.fr, tel: +33140435123

Maria Paola Santisi d'Avila, PhD, Université Paris-Est, Laboratoire Central des Ponts et Chaussées (LCPC), 58 Bd Lefebvre 75732 Cedex 15 Paris (France), santisid@lcpc.fr, tel: +33140435378

Jean-François Semblat, Researcher, Laboratoire Central des Ponts et Chaussées (LCPC), 58 Bd Lefebvre 75732 Cedex 15 Paris (France), semblat@lcpc.fr, tel. +33158357843

Luca Lenti, Researcher, Laboratoire Central des Ponts et Chaussées (LCPC), 58 Bd Lefebvre 75732 Cedex 15 Paris (France), luca.lenti@lcpc.fr, +33140435245

Fabian Bonilla, Researcher, Institute for Radiological protection and Nuclear Safety (IRSN), DEI-SARG department, B.P.17, 92262, Fontenay-aux-Roses Cedex, France, Fabian.bonilla@irsn.fr, tel.+33158357843

ABSTRACT

For moderate or strong seismic events, the maximum strains can easily reach the elastic limit of the soil behavior. Considering soil-structure interaction, the nonlinear effects may change the soil stiffness at the base of the structure and the energy dissipation into the soil. To take into account the nonlinearity of the soil in the dynamic soil-structure interaction (DSSI), a 3D constitutive model, proposed by Iwan, is used to investigate DSSI in the framework of the Finite Element Method. The model accounts for the nonlinear hysteretic behavior of soils and only needs the shear modulus degradation curve to characterize the soil behavior. This feature is very important since complex constitutive models generally involve numerous mechanical parameters difficult to characterize experimentally.

A parametric study is carried out for different types of structures to characterize nonlinear effects in the time domain. Through these numerical simulations, the nonlinear behavior of the soil is shown to have beneficial or detrimental effects on the dynamic response of the structure depending on the way the interaction process is modified: change in the amplitude and frequency content of the waves propagated into the soil, fundamental frequency of the response of the soil-structure system and energy dissipation.

INTRODUCTION

The nonlinear stress-strain behavior of soils can be represented more accurately by cyclic nonlinear models that follow the actual stress-strain path during cyclic loading (Kramer, 1996). Such models are able to represent the shear strength of the soil. A variety of cyclic nonlinear models have been developed; all are characterized by a backbone curve and a series of rules that govern unloading-reloading behavior, stiffness degradation, and other effects. The stress-strain model used in this work is proposed by Iwan (1967)

and used by Joyner and Chen to compute the nonlinear ground response in earthquakes (Joyner and Chen, 1975a). They presented a method based on the Iwan model that takes account of nonlinear, hysteretic behavior of soils and offers considerable flexibility for incorporating laboratory data on soil behavior (Joyner, 1975b). Joyner et al. (1981) improved the model to be capable of generating the energy dissipation in small strain levels.

This form of model has a rich history of application to modeling in the fields of material plasticity, structural

dynamics and vibrations, control systems and magnetics (Segalman and Starr, 2008). After Segalman et al. (2008), what are now often referred to as Iwan might correctly be called Masing-Prandtl-Ishlinskii-Iwan models. They showed that for any material or structural model expressible as a Masing model, there exists a unique parallel-series (displacement based) Iwan system that characterized that model as a function of displacement history.

The Iwan model is used and implemented in the framework of Finite Element to investigate the effect of soil nonlinearity on dynamic soil- structures interaction.

SOIL CONSTITUTIVE MODEL

The soil model initially proposed by Iwan (1967) is used in this work. The model is composed of simple linear springs and Coulomb friction elements arranged as shown in fig. 1.

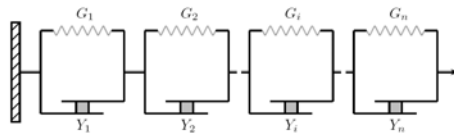


Fig. 1. Iwan model

The friction elements remain locked until the stress exceeds the yield stress Y_i . Generally, the yield stress of the first element Y_1 is set to be zero for simulating the elastic behaviour of the soil. By appropriate specification of the spring constants G_i and the yield stresses Y_i , we can model a very broad range of material behaviour as dictated by laboratory experiments (Joyner, 1975a). The accuracy of the model depends on the number N of elements but it effects the calculation duration and an optimal value should be found.

At any given time, all the elements up to a certain index will be yielding and all those above will not. The Y_i are chosen to cover the range of stresses that the system is expected to encounter and are distributed so that the initial loading curve can be faithfully recovered. From the initial loading curve, a set of shear strain values e_m ($m=1, N+1$) is obtained corresponding to the stress values Y_m . The tangent modulus S_m are then given simply by

$$S_m = \frac{Y_{m+1} - Y_m}{e_{m+1} - e_m} \quad (1)$$

The Iwan model can be used to represent, to any target accuracy, the behaviour of any material whose hysteresis loops satisfy the Masing criterion and do not depend on the number of cycles of loading. Even if a soil does not exactly meet the Masing criterion, its behaviour might still be approximately represented by an Iwan model (Joyner, 1975a). It should be noted that the rheological model used here has no viscous damping, and as a result the stress depends on the

strain (and strain history) but not on the strain rate. Therefore, the energy dissipation per cycle does not depend upon the frequency.

The model initially proposed by Iwan was in 1D but he introduced an extension of the standard incremental theory of plasticity (Fung, 1965). Instead of a single yield surface in stress space, Iwan postulated a family of yield surfaces.

The relationship between mean stress and mean strain is presumed elastic so that

$$de_m = d\sigma_m / 3K \quad (2)$$

where K is the bulk modulus. The deviatoric stress σ_{ij} is considered as a vector in a nine-dimensional space, and a family of yield surfaces is postulated, represented by the yield functions

$$F_n(\sigma_{ij} - \alpha_{ij}) = k_n^2 \quad (3)$$

where k_n is a constant characteristic of the n th surface and α_{ij} represents the origin of the surface. The total deviatoric strain e_{ij} is presumed to consist of the sum of an elastic strain e_{Eij} plus plastic strain components e_{Pij} each associated with the n th yield surface. Kinematic hardening of the Prager type is assumed so that

$$d\alpha_{nij} = C_n de_{Pnij} \quad (4)$$

where C_n is a constant associated with the n th surface.

The plastic strain increments must be normal to the corresponding yield surface. This gives

$$de_{nij} = L_n h_n \frac{\partial F_n}{\partial \sigma_{ij}} \quad (5)$$

where L_n can be 0 or 1 regarding the activity of the unit. The requirement that loading from a plastic state must lead to another state can be used to determine h_n (Fung, 1965)

$$h_n = \frac{1}{C_n} \frac{(\partial F_n / \partial \sigma_{rs}) d\sigma_{rs}}{(\partial F_n / \partial \sigma_{kl}) (\partial F_n / \partial \sigma_{kl})} \quad (6)$$

Summing elastic and plastic strain increment components and substituting from equation (5) and (6) gives the total deviatoric strain increment

$$de_{ij} = Q_{ijrs} d\sigma_{rs} + d\sigma_{ij} / 2G_0 \quad (7)$$

where

$$Q_{ijrs} = \sum_n \frac{L_n (\partial F_n / \partial \sigma_{ij}) (\partial F_n / \partial \sigma_{rs})}{C_n (\partial F_n / \partial \sigma_{kl}) (\partial F_n / \partial \sigma_{kl})} \quad (8)$$

Equation (7) is to be solved for $d\sigma_{rs}$ in terms of de_{ij} , but first it should be noted that only five of the components of $d\sigma_{rs}$ are independent. Then equation (7) is rewritten in terms of the independent components

$$de_{ij} = P_{ij11}d\sigma_{11} + P_{ij12}d\sigma_{12} + P_{ij13}d\sigma_{13} + P_{ij23}d\sigma_{23} + P_{ij33}d\sigma_{33} \quad (9)$$

where (i,j) takes on the values (1,1), (1,2), (1,3), (2,3) and (3,3). The coefficients are given for example by

$$P_{ij11} = \sum_n \frac{L_n (\partial F_n / \partial \sigma_{ij}) (\partial F_n / \partial \sigma_{11} - \partial F_n / \partial \sigma_{22})}{C_n (\partial F_n / \partial \sigma_{kl}) (\partial F_n / \partial \sigma_{kl})} \quad (10)$$

By solving equations (2) and (9), the stress increments are obtained from the strain increments. The coefficients in equation (9) depend on $\partial F_n / \partial \sigma_{ij}$, C_n and L_n . The yield condition of von Mises is used so that

$$F_n = 1/2(\sigma_{ij} - \alpha_{nij})(\sigma_{ij} - \alpha_{nij}) \quad (11)$$

And

$$\frac{\partial F_n}{\partial \sigma_{ij}} = \sigma_{ij} - \alpha_{nij} \quad (12)$$

With that choice, the parameter k_n in the equation that describes the yield surface represents the initial yield stress in simple shear. The values of k_n and C_n are chosen in order to fit laboratory data. It is assumed that the loading curve from an initial state of zero deviatoric stress and strain is known.

In brief, knowing the increment of deviatoric strain, the incremental deviatoric stress can be obtained by multiplying the inverse of the P matrix by the increment of deviatoric strain.

$$d\sigma_{ij} = P_{ijrs} de_{rs} \quad (13)$$

The assumption of an elastic relationship for volumetric stress and strain coupled with the use of the von Mises yielding condition is about the simplest set of choices that could be made. It does not incorporate in any direct way the effects of dilatancy, i.e., the tendency of soils to change in volume when undergoing shear. The effect of dilatancy upon shear strength (through its effect on pore pressure) can be incorporated indirectly, by choosing C_n values that satisfy laboratory data.

NUMERICAL MODEL

The Finite Element code, CESAR-LCPC (Humbert, 2005) is used to simulate the dynamic soil-structure interaction.

The resolution method of the problem of DSSI is based on the discretization in time and space. The second order of implicit

Newmark scheme is used to integrate the equation of motion in time. The unconditional stability factors are considered in all the simulations (0.25 as β and 0.5 as α). The Newton-Raphson algorithm is combined to Newmark scheme for resolution of nonlinear dynamic problem.

Soil model

The constitutive soil model, explained in previous section initially studied separately to investigate its rheological behaviour for different strain levels. Figure 2 shows the stress-strain curve for a single component sinusoidal strain with increasing amplitude (Simple shear loading). It means that only the ε_{xz} and ε_{zx} members of the strain matrix are nonzero.

The red line shows the monotonic loading curve, known as the backbone curve.

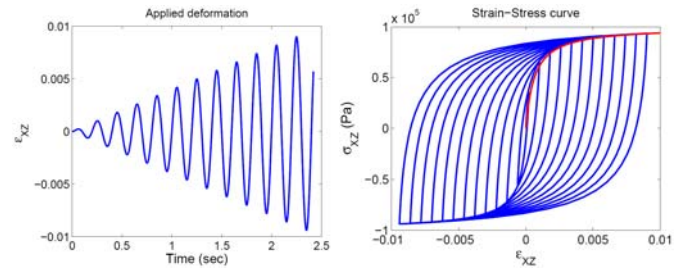


Fig. 2. Stress-Strain curve (Simple shear loading)

The results are satisfactory and the loading and unloading cycles are coherent with the backbone curve. On the other hand, stress-strain cycles computed by the model do not reach the ultimate strength of the material at the level of strain that the earthquakes occur.

Another example consists in a 3D response of the model by using a sinusoidal strain for all components with different increasing amplitudes. In this case, the strain matrix is composed of fully nonzero members. Figure 3 shows the stress-strain curve in the xy, xz and yz directions.

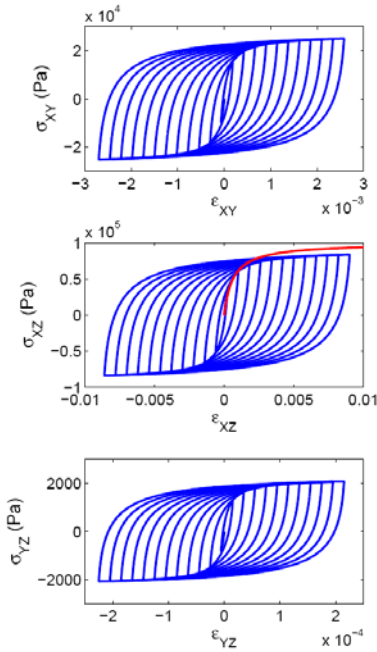


Fig. 3. Stress-strain curve in xy , xz and yz direction

We can observe that the model is also capable to generate the hysteresis curve, and the material strength is less than that obtained for simple shear loading (one component). It means that the level of nonlinearity is more important in this case.

Seismic excitation

The stress-strain cycles are shown in fig. 4 for simple shear loading due to the Loma Prieta earthquake (1989). In this case we have non uniform loading and unloading, the model generates the hysteresis cycles by following the Masing rules and respecting the ultimate resistance of the soil.

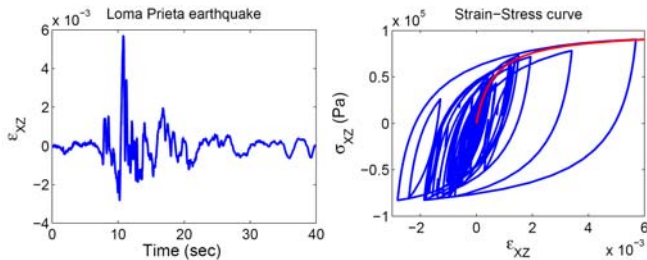


Fig. 4. Stress-strain curve for Loma Prieta earthquake

In the next step, the model is implemented at the framework of the Finite Element method (CESAR-LCPC code), and non linear seismic wave propagation is investigated.

Boundary condition

The borehole condition is considered at the base of the soil model. It means that at the level of applied input motion, total displacement is equal only to the incident wave. For the lateral boundaries the periodic condition is supposed. Consequently,

the displacement, strain and stresses are equal on both lateral boundaries. We need to have a large domain to obtain accurate results.

NON LINEAR WAVE PROPAGATION AND VALIDATION OF THE MODEL

Validation of the model

Our numerical results (Iwan model, FE) are now compared to the linear equivalent, EERA (Bordet et al., 2000), nonlinear NERA, (Bordet and Tobita, 2001) numerical results and a Finite Difference (Bonilla, 2000) program based on nonlinear Iwan model (Iwan model, FD). All the three codes are based on Finite Difference. EERA is a computer program starting from the same basic concepts as SHAKE and it stands for equivalent-linear earthquake response analysis. NERA is a non-linear site response analysis program based on the material model developed by Iwan (1967).

A 1D single soil layer of 50m (fig. 5) is supposed to compare the nonlinear wave propagation results between the different approaches. The density of the soil is 1900 kg/m^3 and the shear wave velocity in soil is 150 m/s . The shear modulus reduction curve vs. cyclic shear strain is shown in fig. 5.

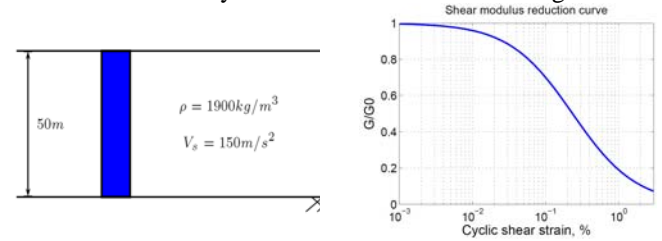


Fig. 5. Geometrical and material properties of the soil layer

The Ricker wavelet of order zero, Gaussian wavelet (Semblat and Pecker, 2009), is applied at the base of the soil layer with three different PGAs (0.0075, 0.15, 0.5 g) to have a wide range of nonlinearity (fig. 6).

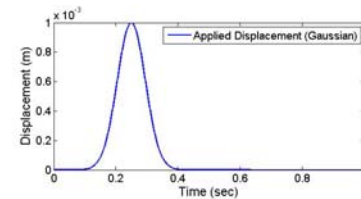


Fig. 6. Ricker wavelet of order zero

The 1D simulations are performed for different strain levels. The total duration of the simulations is 20 seconds. The acceleration obtained at the surface of the soil column is compared between our model (FE), EERA, NERA and Iwan model (FD) for PGA equal to 0.15g (Fig. 7).

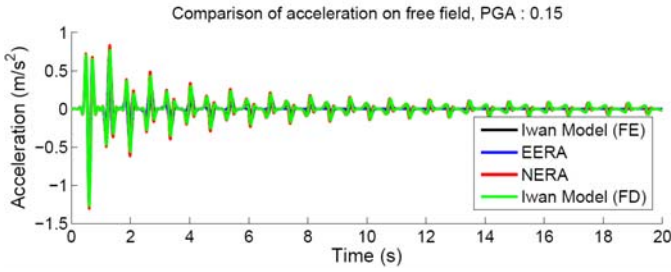


Fig. 7. Acceleration at free field for PGA : 0.15g

We can observe that the results are satisfactory during the propagation process. To have a better idea of the differences between the results, fig. 8 shows the results for only the first second (first acceleration peak) of wave propagation for three different levels of input motion.

As we can see in fig. 8, top-left, the results are very close for a PGA equal to 0.0075g (low strain level) the accelerations are very close. For moderate strain (fig. 8, top-right), there is a slight difference between the results and finally for large strain level (fig. 8, bottom) there is a significant difference between the accelerations at the surface of the soil column obtained by these numerical tools. In all three cases, the acceleration obtained at the surface of the soil column by Iwan model (FE), is smaller than that obtained from the three other programs. It means that our nonlinear FE model is more dissipative when compared to the three other numerical tools. We can observe the same result by comparing the arrival time of peak acceleration, which shows the velocity of the propagation is slower for the implemented Iwan model (FE).

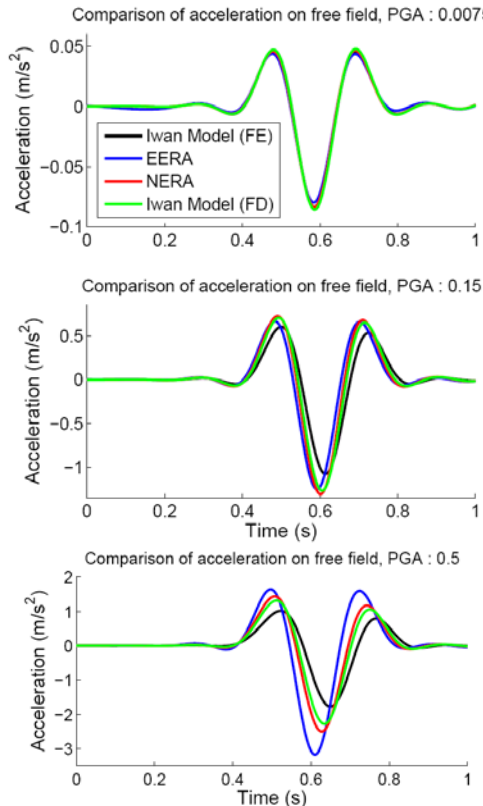


Fig. 8. Comparison of acceleration between the four programs for the first second of the propagation

The difference between the results is partially due to the nature of the resolution method used in these numerical tools (Finite Element and Finite Difference). We should also take into account the differences between the time and spatial discretization chosen in each case.

The transfer function is also compared for our model, EERA and NERA programs. The transfer function is the ratio of the free field acceleration and the input motion at the base of the soil layer. The results in frequency domain are displayed in fig. 9. For small strain level (PGA equal to 0.0075g), close to the elastic behaviour of the soil, the fundamental frequencies of the soil layer obtained by our model (FE) and EERA are more realistic specially when compared to the theory. For large strain level, the frequencies obtained by our model are closer to NERA (fully non linear program) than EERA.

Wave propagation for different strain levels

The acceleration, velocity and displacement at the surface of the soil layer obtained by our model are compared for different levels of strain (fig. 10). The left column in fig. 10 displays the results for PGA of the input motion equal to 0.0075, 0.015, 0.075 and 0.15g and in the right column we have the same results for PGA equal to 0.2, 0.3, 0.4 and 0.5g. It is obvious that, for increasing strain levels, the nonlinearity increases (apparent wave velocity decreases) and much more energy is dissipated. In fig. 10, we can observe that the residual displacement increases for increasing strain level.

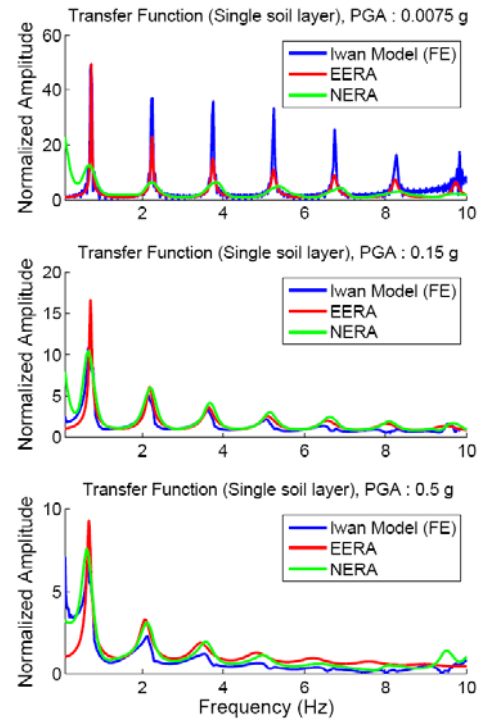


Fig. 9. Comparison of the transfer function obtained by three programs for PGAs: 0.0075, 0.15 and 0.5g

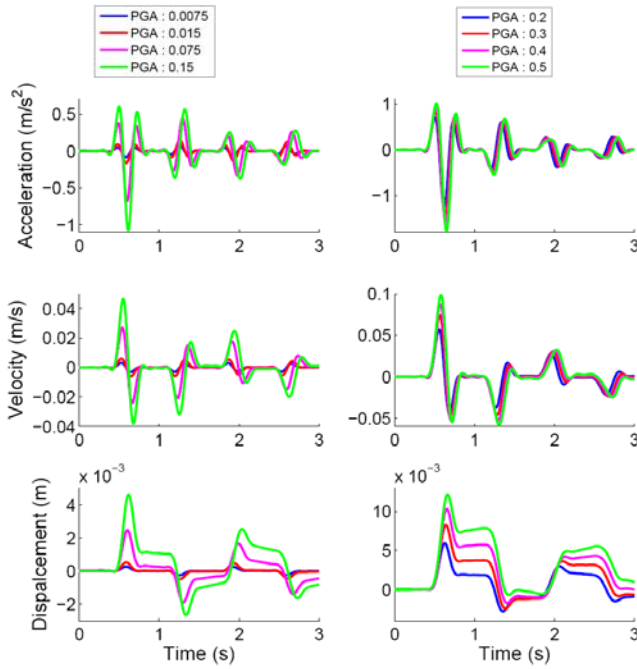


Fig. 10. Acceleration, velocity and displacement at the surface of the soil layer for different PGAs

In order to observe the level of nonlinearity, the input acceleration at the base of the soil layer versus the output acceleration obtained at the surface of the soil for different PGAs is shown in fig. 11. It can be noticed that the ground motion is amplified for a moderate input motion. When the strain level increases, the effect of soil nonlinearity is larger and involves stronger energy dissipation. That is, a part of the energy is dissipated in the soil before reaching the surface and therefore, the seismic motion is strongly attenuated.

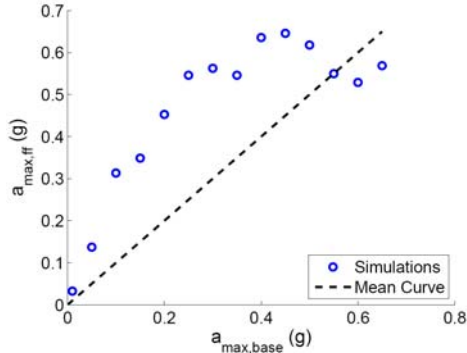


Fig. 11. Input acceleration vs. free field acceleration

Comparison of 1D and 2D simulations

We compare also the results of a single soil layer in one and two dimensions. The 2D finite element model consists of 50 meters deep and 250 meters long. The soil properties are exactly the same as 1D model (Fig. 12).

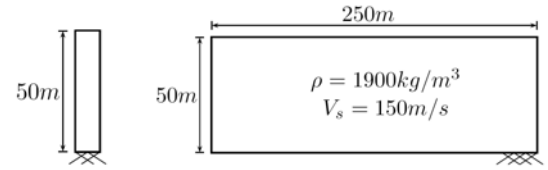


Fig. 12 : 1D and 2D model properties

A Ricker wavelet of order zero is applied as input motion in horizontal direction and the acceleration, velocity and displacement are compared at the surface of the soil (fig. 13).

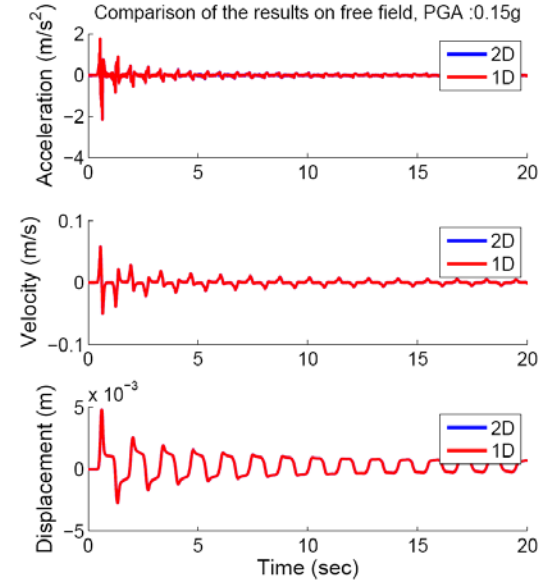


Fig. 13. Comparison between 1D et 2D model

As we expect the results are the same.

NON LINEAR DYNAMIC SOIL-STRUCTURE INTERACTION

The effect of soil nonlinearity is now investigated by means of the Iwan model implemented in the finite element method (CESAR-LCPC code).

Structural model

As the main objective of this paper is to study the effect of nonlinearities of the soil on the DSSI, the elastic material behaviour is considered for the structures. The structures (table 1) are modelled by 2D frames with one span and one floor (Fig. 14). The columns are massless and the beams have a large stiffness.

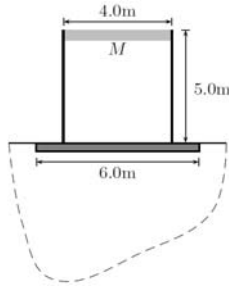


Fig. 14. Structural model

The flexibility of the foundations is not taken into account (rigid foundations).

Table 1. Fundamental frequency of the various structures

N.	Mass of the beam (t/m^3)	Fund. Frequency (Hz)
1	5	3.3937
2	8.5	2.6124
3	23.5	1.5764
4	24.5	1.544
5	25.5	1.5136
6	28	1.4446
7	50	1.0818

Soil model

The soil is composed of 5 layers with five different material properties (fig.15). The shear modulus reduction curve versus cyclic shear strain for different layers is shown in fig. 16.

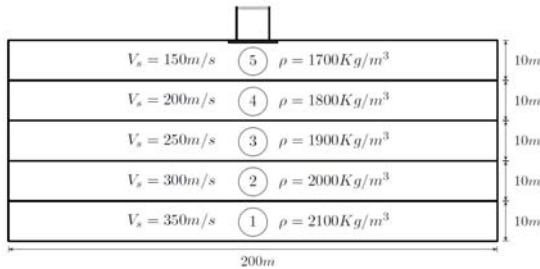


Fig. 15. Soil-structure model

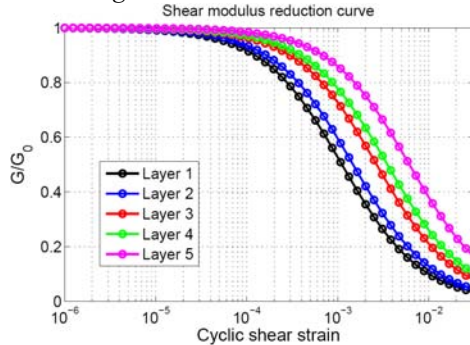


Fig. 16. Shear modulus reduction curve (hyperbolic model) in the various soil layers

The foundation and the soil are perfectly connected and the sliding and uplift of the foundation are not considered.

Soil-Structure interaction

To study the nonlinearity of the soil, the soil-structure model is excited by Ricker wavelet (order zero) with various amplitudes. The nonlinear response of the soil-structure system is compared to its linear response. Acceleration, velocity and displacement at the top of the structure are compared for different input motions (PGA equal to 0.1, 0.25 and 0.5g) in fig. 17 for the frame with the fundamental frequency equal to 1.4446 Hz (structure 6) for the first 5 seconds of the analysis. We can observe that the amplitude of the acceleration and velocity decrease especially for PGA equal to 0.5g. The soil nonlinearity causes some residual displacement. Because of soil nonlinearity a part of the energy dissipates into the soil before reaching the structure and therefore the amplitude at the top of the structure is smaller.

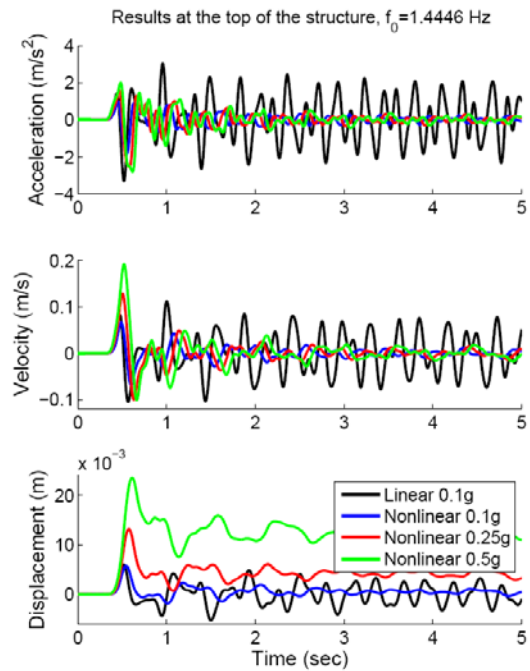


Fig. 17. Response of the structure 6 to Ricker excitation

To see better the results, only the first second of acceleration is shown in fig. 18. By comparison to the first acceleration peaks obtained at the top of the structure, the amplitudes for all nonlinear cases are less than in the linear case with an input PGA equal to 0.1g. It means that the effect of nonlinearity is very significant. The apparent wave velocity is also different for these four cases; we can observe that it decreases for increasing soil nonlinearity.

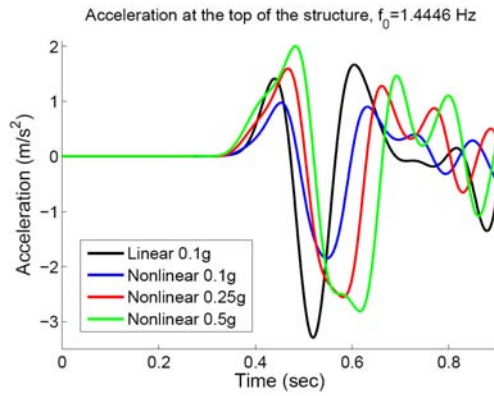


Fig. 18. First second of acceleration at the top of structure

The Fourier transform of the displacement at the top of this structure for all the different cases is shown in fig. 19. The fundamental frequency of this frame on fixed base is 1.4446 Hz. As we can see the first natural frequency of the soil profile (linear behavior) is 1.48 Hz. By considering the soil-structure interaction with linear behavior of the soil the fundamental frequency of the system shifts to the low frequency and is equal to 1.358 Hz. It means that we have 6% of frequency reduction. By considering the nonlinear behavior of the soil, the fundamental frequency of the system keeps decreasing and it changes from 1.343 Hz (PGA equal to 0.1g) to 1.328 Hz (PGA equal to 0.5g).

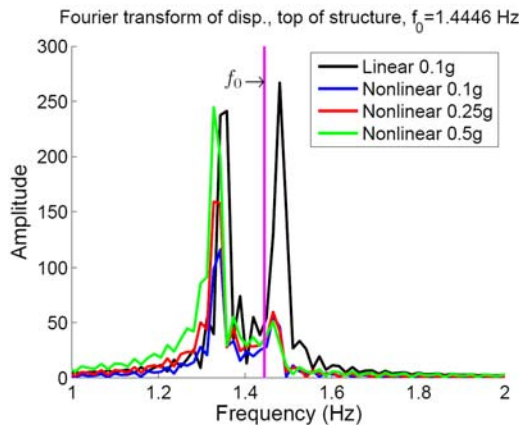


Fig. 19. Fourier transform of the displacement (structure 6)

It means that the fundamental frequency decreases again 2.2% for the nonlinear soil with PGA equal to 0.5g in comparison with linear behavior of the soil.

The same results are studied for the structure with the fundamental frequency on fixed base equal to 2.6124 Hz (structure 2). The acceleration, velocity and displacement at the top of the structure are shown in fig. 20. In this case also we have a significant reduction of the structural response because of the soil nonlinearity.

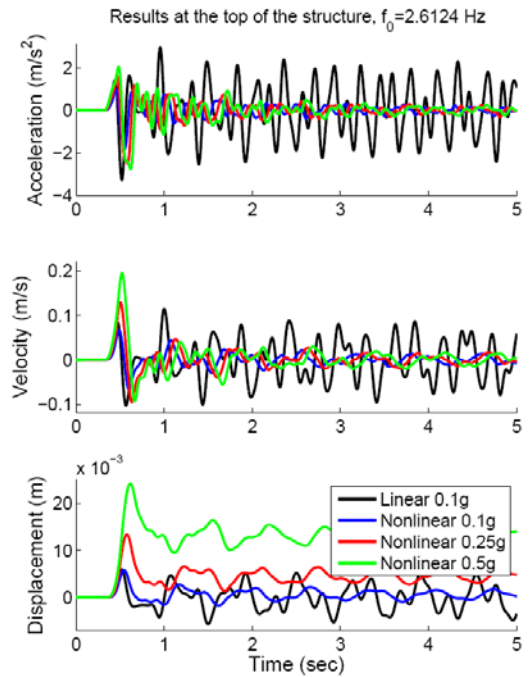


Fig. 20. Response of the structure 2 to Ricker excitation with various PGAs

The first second of acceleration at the top of the structure is shown in fig. 21. We can observe the energy dissipation in the soil and its effect on the acceleration amplitude at the top of the structure and the apparent wave velocity.

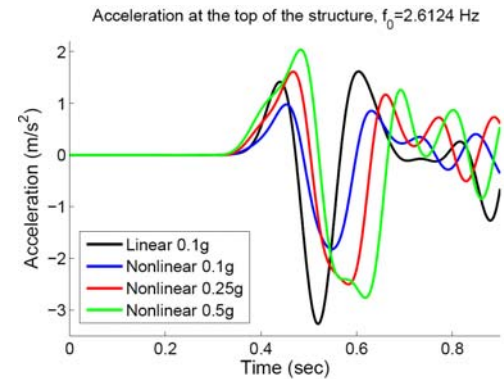


Fig. 21. First second of acceleration at the top of the structure

The Fourier transform of the displacement at the top of the structure is shown in fig. 22. As we know the fundamental frequency of the structure on fixed base is 2.6124 Hz. By considering the soil with linear behavior, the fundamental frequency of the system decreases until 2.487Hz, that is, 4.8%. For the nonlinear case, PGA equal to 0.5g, it reaches 2.472 Hz. It means that the frequency is decreased by 2.7% when compared to the linear behavior of the soil. We can observe that the decrease of fundamental frequency of the soil-structure system of two structures (structures 2 and 6) is different.

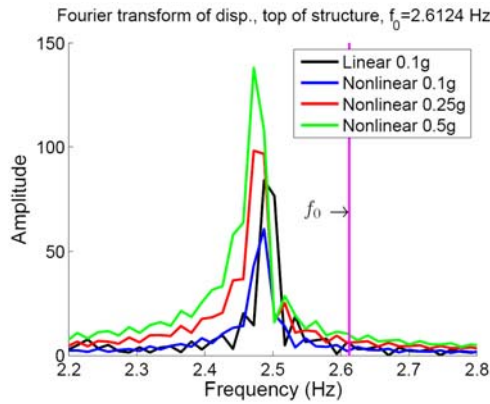


Fig. 22. Fourier transform of the displacement (structure 2)

The only difference between these two frames is the mass of the structures. Also, as we know, we can have the same fundamental frequency (on fixed base) with different geometrics, rigidities and masses of the structures. Furthermore, we will study the effect of these differences.

Soil response

It is now necessary to study what happens in the soil, which causes the reduction of the response of the structure. The hysteresis cycles at different soil layers are shown in fig. 23 for the soil-structure model with fundamental frequency of the structure equal to 1.0808 Hz on fixed base (structure 7).

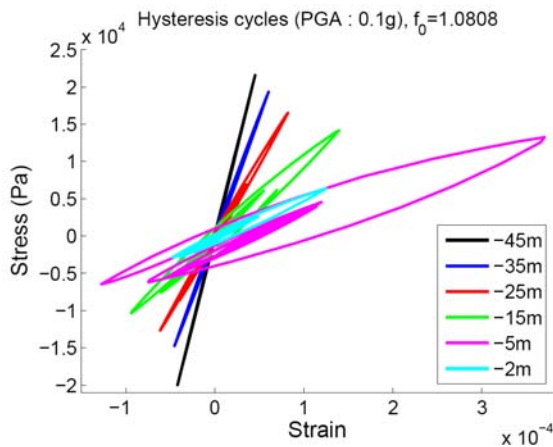


Fig. 23. Hysteresis cycles at different soil layers (PGA : 0.1g)

As the dissipated energy is related to the surface of the cycles of the stress-strain curve, we can observe that the energy dissipation is more significant for the layer close to the surface of the soil (5m to the surface). In this case the maximum shear strain reaches to 0.04%. The soil behavior remains elastic in layers 1 and 2. The results are coherent with the shear modulus reduction curve of the profile of the soil shown in fig. 16.

By increasing the amplitude of the input motion, we expect more nonlinearity. Figure 24 shows the hysteresis cycles of the same soil-structure model (fundamental frequency of the

structure on the fixed base equal to 1.0808 Hz) for input motion with PGA equal to 0.5g.

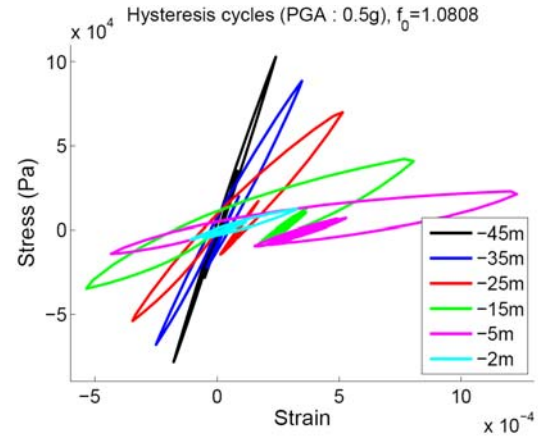


Fig. 24. Hysteresis cycles at different soil layers (PGA : 0.5g)

In this case the nonlinearity in the soil layer 1 is obvious. The shear strain in the soil layer 5 (5m from the surface) reaches up to 0.12%. For this strain level the energy dissipation is larger than with a 0.1g PGA. That is why the accelerations are approximately equal at the top of the structure despite the large difference between the input motions (fig. 18 and 21).

Structural response

For the seven structures of table 1, the normalized maximum acceleration at the top of the structure is shown versus normalized frequency of the structures (fig. 25). The maximum acceleration at the top of the structure is normalized by the maximum acceleration of the input motion (PGA). The fundamental frequency of the structures (fixed base) is normalized by the first natural frequency of the soil (1.48 Hz). By considering the nonlinear behavior of the soil, the input motion with a 0.5g PGA leads to a lower amplification than the 0.1g PGA in all cases because the nonlinearity in the soil layers is larger. For the higher normalized frequency (structure 1), the amplification in nonlinear cases is larger. It should be noticed that the mass of the structure is the only difference between these seven structures and higher normalized frequency means smaller mass of the structure.

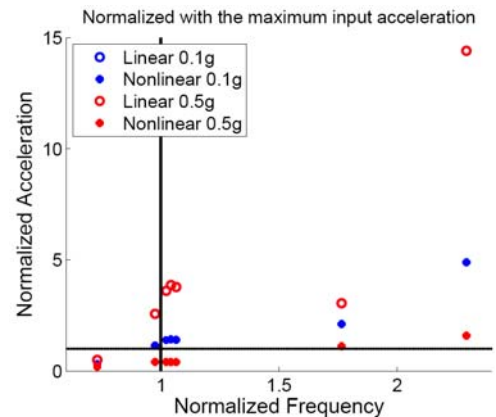


Fig. 25. Normalized acceleration vs. normalized frequency

By decreasing the normalized frequency and considering the nonlinear behavior of the soil, the acceleration at the top of the structure is less than the input motion. In fig. 26, the same results are analyzed considering another definition of the normalized acceleration. In this case, the maximum acceleration is normalized by the maximum acceleration of the corresponding linear case. The acceleration strongly decreases for the normalized frequency close to 1. It should be noticed that these results are only for the structural type that we considered and may be different for other types of structure.

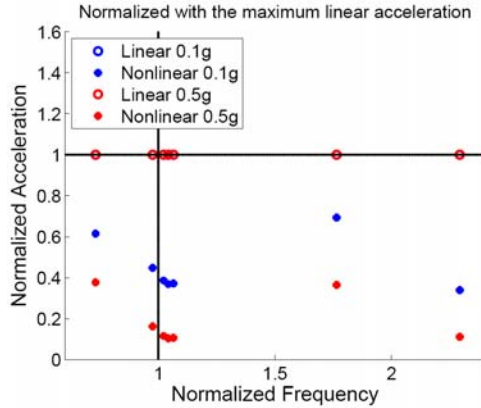


Fig. 26. Normalized acceleration vs. normalized frequency

The same graphs are shown in fig. 27 and 28 for normalized displacement. In fig. 27, the maximum displacement at the top of the structure is normalized by the maximum displacement of the input motion. The normalized displacement in the linear case is larger than other cases for the normalized frequency close to 1, that is, for the structures with fundamental frequencies close to the natural frequency of the soil. It means that we have the resonance in the system.

By comparing the results in fig. 25 and fig. 27, we notice that the maximum normalized acceleration for the 0.5g PGA input motion is less than for 0.1g, but the maximum normalized displacement for 0.5g PGA is larger than that of 0.1g.

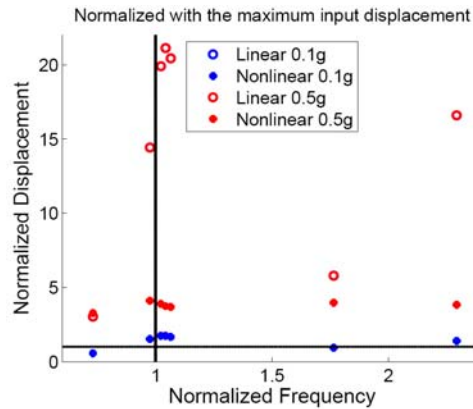


Fig. 27. Normalized displacement vs. normalized frequency

We may conclude that the acceleration is more influenced by soil nonlinearity.

In fig. 28, the normalized displacement is obtained by normalizing the maximum displacement at the top of the structure by the corresponding linear maximum displacement. We observe that for the normalized frequency close to 1 the nonlinearity is more significant and the maximum normalized displacement is less than other structure except for the highest normalized frequency (structure 1). It means that the mass of the structure is also very important.

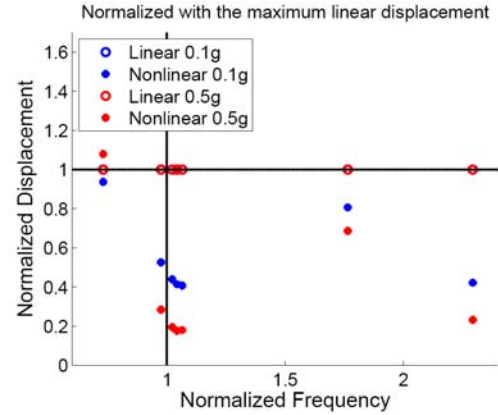


Fig. 28. Normalized displacement vs. normalized frequency

Effect of structural properties at soil-structure response

To study the effect of the mass of the structure, another example is investigated with a huge mass but with the same fundamental frequency as structure 6. The geometry of this frame is different. The height of this frame is equal to 10m but its width is the same. The total mass of this structure is more than 50 times the total mass of structure 6, and obviously the stiffness of the columns should be larger than that of other structures to have the same fundamental frequency. Acceleration, velocity and displacement at the top of the structure for the first 5 seconds are shown in fig. 29. In this case, we also noticed the effect of soil nonlinearity on the response of the structure.

Figure 30 shows the Fourier transform of the acceleration at the top of the structure. The fundamental frequency of the structure on fixed base is equal to 1.4441 Hz (equal to fundamental frequency of structure 6). By considering soil-structure interaction the fundamental frequency of the system decreases down to 0.4578 Hz for linear behavior of the soil. It means that the fundamental frequency is divided by three. By considering the soil nonlinearity this frequency reaches to 0.217 Hz, that is, the fundamental frequency is divided by two.

Despite the very large values chosen for the parameters, it shows that the structural model and the mass of the structure are very important and may significantly change the response of the structure by considering nonlinear behavior of the soil.

CONCLUSIONS

The Iwan model is implemented at the framework of the Finite Element method (CESAR-LCPC code), and nonlinear seismic wave propagation especially for the problem of dynamic soil-structure interaction is investigated.

We observe that, because of soil nonlinearity a part of input energy (depending to the strain level) dissipates in soil before reaching the surface. Consequently, the response amplitude of structure such as acceleration, velocity and displacement at the top of the structure decreases.

Considering soil nonlinearity, the fundamental frequency of the soil-structure system decreases compared to the structure based on a linear soil.

The total mass of the structure is a very important factor that influences the reduction of fundamental frequency of soil-structure interaction.

The response of the structure such as acceleration and displacement at the top of the structure is more influenced of soil nonlinearity for the structure with the fundamental frequency close to the natural frequency of soil.

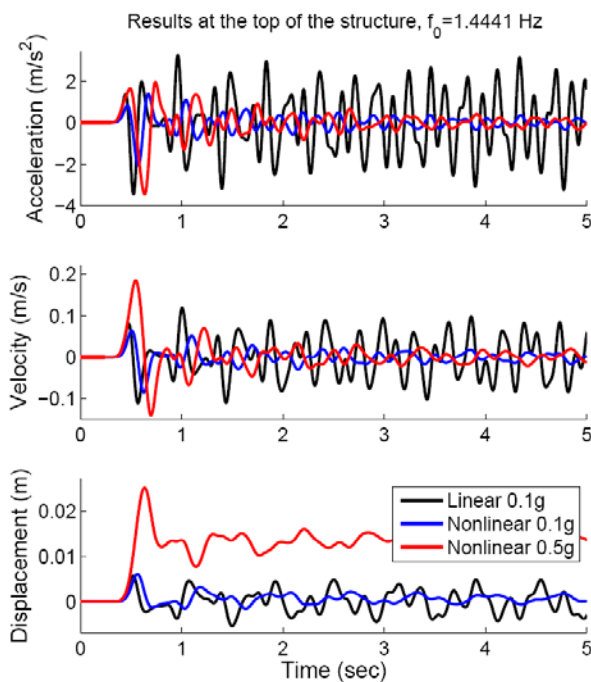


Fig. 29. Acceleration, velocity and displacement at the top of the structure

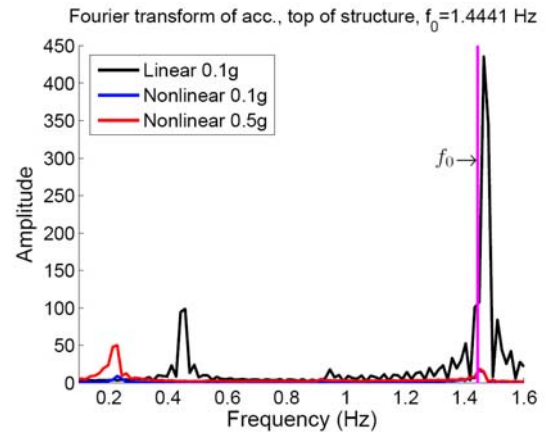


Fig. 30. Fourier transform of the acceleration at the top of the structure

REFERENCES

- Bonilla L. F. [2000], "Computation of linear and nonlinear site response for near field ground motion", Dissertation for PhD degree, University of California, Santa Barbara
- Cacciola C. et al. [2009], "Site response analysis using the Preisach formalism", *Pro. Of Twelfth Int. Conf. on Civil Struc. And Environmental Eng. Computing*, B.H.V. Topping, L.F. Costa Neves and R.C. Barros, Civil-Comp Press, Stirlingshire, Scotland
- Bardet J. P., Ichii K. and Lin C. H. [2000], "EERA, A computer program for Equivalent-linear Earthquake site Response Analyses of Layered Soil Deposits", University of Southern California
- Fung, Y. C. [1965]. "Foundation of solid mechanics". Prentice-Hall, Englewood Cliffs, New Jersey
- Humbert P., Dubouchet A., Fezans G. and Remaud D. [2005], "CESAR-LCPC, un logiciel de calcul dédié au génie civil", *Bul. Des Laboratoires des Ponts et Chaussées*, N. 256-257
- Iwan, W. D. [1967]. "On a class of models for the yielding behaviour of continuous and composite systems". *J. Appl. Mech.*, No 34, pp. 612-617
- Joyner W. B. and Chen A. T. F. [1975a]. "Calculation of nonlinear ground response in earthquakes". *Bul. of the Seismological Society of America*, Vol. 65, No. 5, pp 1315-1336
- Joyner W. B. [1975b]. "A method for calculating nonlinear seismic response in two dimensions". *Bul. of the Seismological Society of America*, Vol. 65, No. 5, pp 1337-1357

Joyner W. B., Warrick R. E. Ad Fumal T. E. [1981], *“The effect of quaternary alluvium on strong ground motion in the Coyote lake, California, earthquake of 1979”*, Bul. of the Seismological Society of America, Vol. 71, No. 4, pp 1333-1349

Kramer S. L. [1996], *“Geotechnical Earthquake Engineering”*, Prentice-Hall, Inc.

Lenti L. [2006], *“Modellazione di effetti non lineari in terreni soggetti a carico ciclico e dinamico”*, Thesis in Geophysics, University of Bologna (Italy)

Bardet J. P. and Tobita T. [2001], *“NERA, A computer program for Nonlinear Earthquake site Response Analyses of Layered Soil Deposits”*, University of Southern California

Segalman, D. J. and Starr M. J. [2008]. “Inversion of Masing models via continuous Iwan systems”, Int. J. of Non-linear Mec., N. 43, pp. 74-80.

Semblat J-F. and Pecker A. [2009], *“Waves and Vibrations in Soils: Earthquakes, Traffic, Shocks, Construction works”*, IUSS press